adsorption isotherms recorded on a Micromeritics ASAP 2000 porosimeter. Surface areas were determined by the BET method; pore volumes were obtained from single-point measurements at a normalized partial pressure (P/P_o) of 0.9837. Pore-size distributions were determined by the Barrett-Joyner-Halenda (BJH) method. The accuracies of the BJH and BET methods in this small size regime are limited, and, therefore, the resulting pore-size distributions and surface areas should be considered approximate.
31. A $d_{(100)}$ spacing of 30 Å corresponds to a lattice constant *a* of $2d/\sqrt{3}$ or 35 Å.
32. L. Powers and P. S. Pershan, *Biophys. J.* **20**, 137 (1977); L. Powers and N. A. Clark, *Proc. Natl. Acad. Sci. U.S.A.* **72**, 840 (1977); G. G. Barclay, S. G. McNamee, C. K. Ober, K. I. Papathomas, D. W. Wang, *J. Polym. Sci. Part A Polym. Chem.* **30**, 1845 (1992); M. Lukaschek, D. A. Grabowski, C. Schmidt, *Langmuir* **11**, 3590 (1995); J. A. Müller, R. S. Stein, H. H. Winter, *Rheol. Acta* **35**, 160 (1996).
33. P. A. Winsor, in *Liquid Crystals and Plastic Crystals*, G. W. Gray and P. A. Winsor, Eds. (Ellis Harwood, Chichester, UK, 1974), vol. 2, pp. 122–143; K. Amundson, E. Helfand, X. Quan, S. D. Hudson, S. D. Smith, *Macromolecules* **27**, 6559 (1994).
34. A. M. Figueredo Neto and L. Q. Amaral, *Mol. Cryst. Liq. Cryst.* **74**, 109 (1981).
35. H. Gutman, Z. Luz, E. J. Wachtel, R. Poupko, J. Charvolin, *Liq. Cryst.* **7**, 335 (1990); M. Jansson, R. L. Thurmond, T. P. Trouard, M. F. Brown, *Chem. Phys. Lipids* **54**, 157 (1990); H. Gutman, A. Loewenstein, Z. Luz, R. Poupko, H. Zimmermann, *Liq. Cryst.* **9**, 607 (1991); W. Schnepp, S. Disch, C. Schmidt, *ibid.* **14**, 843 (1993).
36. Q. Huo and G. D. Stucky, manuscript in preparation.
37. Q. Huo, R. Leon, P. M. Petroff, G. D. Stucky, *Science* **268**, 1324 (1995).
38. G. S. Attard, J. C. Glyde, C. G. Göltner, *Nature* **378**, 366 (1995).
39. Some cationic surfactant is expelled from the composite as the anionic silica charge density is reduced because of polymerization (*22*). The crystalline CTAB peaks are oriented because the plate-like crystals tend to lie flat on the surfaces of the bulk composite.
40. Powder Diffraction File entry 80-1746 (International Center for Diffraction Data, Newtown Square, PA, 1992).
41. P. I. Ravikovitch, S. C. Odomhnaill, A. V. Neimark, F. Schüth, K. K. Unger, *Langmuir* **11**, 4765 (1995).
42. Supported by NSF grants CHE-9626523 (S.H.T.), DMR-9520971 (G.D.S.), and DMR-9257064 (B.F.C.); the U.S. Army Research Office (DAAH04-96-1-0443); a Henkel Foundation–American Chemical Society Research Fellowship in Colloid and Surface Chemistry (A.F.); the David and Lucile Packard Foundation (B.F.C.); and Shell Research B.V. (B.F.C.). This work made use of instrumentation supported in part by the NSF Division of Materials Research under grant DMR-922257 and through the University of California, Santa Barbara, Materials Research Laboratory under award DMR-9632716. B.F.C. is a Camille and Henry Dreyfus Teacher-Scholar and an Alfred P. Sloan Research Fellow.

3 July 1997; accepted 29 August 1997

The Response of Jupiter's Magnetosphere to an Outburst on Io

Michael E. Brown* and Antonin H. Bouchez

A 6-month-long monitoring campaign of the Io plasma torus and neutral cloud was conducted to determine the characteristics of their interaction. During the observations, a large outburst of material from Io—inferred to be caused by the eruption of a volcanic plume on Io—caused a transient increase in the neutral cloud and plasma torus masses. The response of the plasma torus to this outburst shows that the interaction between Io and Jupiter's magnetosphere is stabilized by a feedback mechanism in which increases in the plasma torus mass cause a nonlinear increase in loss from the plasma torus, limiting plasma buildup.

Jupiter's magnetosphere is filled with plasma mostly derived from Io, the innermost of the large satellites of Jupiter and the most volcanically active body in the solar system. The magnetospheric plasma and the volcanos on Io are tightly coupled: the volcanos feed material, primarily S and O, to the atmosphere and surface frosts of Io (*1*); bombardment by magnetospheric plasma removes the atmosphere and frosts into an extended cloud of gas surrounding the satellite's orbit (*2*). This gas is ionized by collisions with the magnetospheric plasma, becomes incorporated into the Io plasma torus (the inner, dense portion of the jovian magnetosphere), and returns to further bombard Io.

The plasma density in the Io plasma torus remained roughly constant over at least a 13-year period (*3*), even though volcanic activity on Io is presumably sporadic (*4*). The stability of the system in the face of variable volcanic input must be achieved through some feedback mechanism, either through the regulation of supply to the extended gas cloud surrounding Io ("supply-limited") or through regulation of loss from the plasma torus ("loss-limited") (*5*, *6*).

The system will be supply-limited if an increase in the plasma bombardment rate causes a less strong increase in the rate of supply to the extended neutral gas cloud. Two atmospheric models that lead to supply-limitation include an ionospheric buffering model, where an increase in plasma bombardment increases Io's ionosphere, which then begins to deflect the plasma bombardment, thus reducing the supply of material to the neutral cloud (*7*), and a constant-source model, where supply to the neutral cloud is a characteristic solely of Io's atmosphere and does not change with changing plasma bombardment (*8*).

The system will be loss-limited if increases in plasma mass cause even larger increases in plasma loss. One loss-limited plasma transport model suggests that depletion of the plasma torus is driven by nonlinear centrifugally driven diffusion caused by the fast rotation of the jovian magnetosphere. In such a system, the diffusion rate is proportional to the square of the plasma density (rather than to the first power of the density for linear diffusion) (*9*). Another loss-limiting mechanism could be plasma transport initiated by large-scale plasma instability (*10*), where the onset and growth of the instability would lead to a nonlinear plasma loss.

To determine the type of feedback mechanism operating on Io (Fig. 1), we monitored emission from the Io plasma torus and the extended neutral cloud of material surrounding Io's orbit for 6 months. We report a major perturbation to the system that occurred in March 1992, most likely as a result of a volcanic outburst on Io.

We observed S^+ in the Io plasma torus and Na in the extended neutral cloud on 56 clear nights between 1 December 1991 and 1 June 1992, using the Lick Observatory 0.6-m coudé auxiliary telescope connected to the Hamilton echelle spectrograph (*11*). These two species were chosen because they have the brightest emission intensities in the visible wavelength range for a plasma torus ion (S^+) and neutral cloud atom (Na). About 10% of the plasma torus at a distance of 6 R_J is composed of S^+ (*12*). Sodium is about 100 times less abundant than S or O in the neutral cloud (*2*), but we will attempt to use it as a tracer of the major species. From these spectra, we extract emission intensity as a function of distance from Jupiter along the entire slit and compare the behavior of S^+ from the plasma torus and Na from the neutral cloud (Fig. 2) (*13*).

A sudden increase in the brightness (and thus, mass) of the neutral Na cloud started around Julian date 2448680, or 27 February 1992 (hereafter, only the last three digits of each Julian date will be given), followed by a more gradual increase in the plasma torus emission intensity. The Na cloud mass increased by an average of about a factor of 2 for at least 65 days, with transient increases of higher than a factor of 4. The S^+ plasma

Division of Geological and Planetary Sciences, California Institute of Technology, Pasadena, California 91125, USA.

*To whom correspondence should be addressed. E-mail: mbrown@gps.caltech.edu

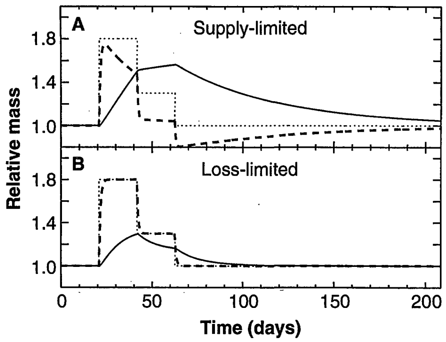

Fig. 1. Models of the response of the extended neutral cloud of Io and the Io plasma torus to a volcanic outburst on Io (*22*). The dotted line indicates the volcanic input, including a two-step, 40-day outburst for illustrative purposes. The dashed line shows the neutral cloud mass, and the solid line shows the plasma torus mass. In both models, the neutral cloud mass responds quickly to the outburst, because the lifetime in the neutral cloud is less than a day (*25*). The plasma torus mass responds more slowly because the plasma lifetime is of the order of 50 days (*26*). (**A**) The supply-limited case. (**B**) The loss-limited case.

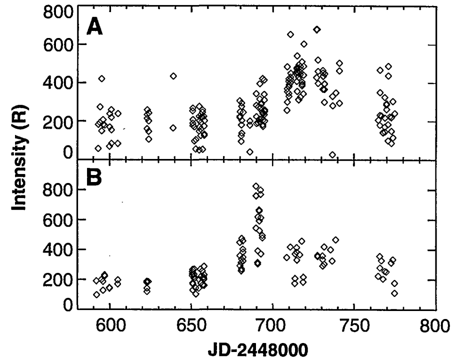

Fig. 2. The intensity of (**A**) 673.1 nm S^+ emission from the plasma torus and (**B**) 589.0 nm Na emission from the neutral cloud as a function of Julian date. The observations begin on 1 December 1991, which is JD 2448591. Intensities are in Rayleighs, defined as 1 R = $[1/(4\pi)] \times 10^6$ photons cm^{-2} s^{-1} sr^{-1}. Typical measurement errors for the data are ~20%. Scatter beyond this amount is caused by the intrinsic variability of the plasma torus and neutral cloud.

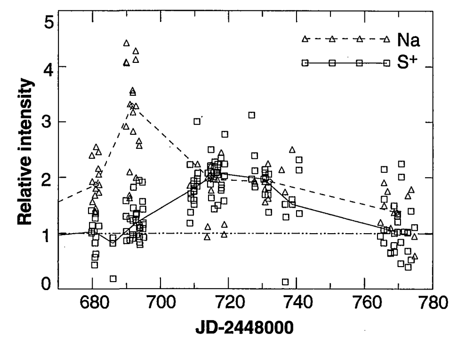

Fig. 3. A direct comparison of the neutral Na and ionized S emission intensities. Both are plotted relative to the median of their preoutburst values. The data are connected by lines through the median values of the seven separate clusters of data.

torus mass increased by almost 30% over this time period and dropped back to its previous value after the Na outburst (Fig. 3) (*14*). The timing of the neutral cloud and plasma torus perturbations is evidence that an increase in mass injection from Io caused the neutral cloud perturbation, which then caused the plasma torus perturbation. For example, on day 680, the Na mass had already increased by a factor of 2, while all observations showed that the plasma torus remained undisturbed. The simplest explanation for this observation is that the mass supply to the neutral cloud suddenly doubled. The plasma torus intensity slowly began increasing around this time, and an extrapolation of the increasing phase of the plasma torus perturbation suggests a starting time around day 685. Such behavior would be expected from an increase in injection of material from Io starting around day 680 (*15*).

In a purely supply-limited system, the plasma torus mass must increase any time the neutral cloud mass is above its equilibrium value (Fig. 1). This requirement results because supply to the plasma torus is proportional to the ionization and charge-exchange rates, which are proportional to the product of the plasma and neutral densities, whereas loss is proportional only to the plasma density. Figure 3 shows that the system does not respond in this supply-limited manner; from day 705 until day 740, the neutral Na cloud was about twice as massive as it was before the outburst, but the plasma torus decreased in mass by 20%. Such behavior can only be achieved in a loss-limited system. The system maintains stability by a nonlinear increase in plasma loss as the plasma torus mass increases. This increased loss overcomes the supply rate increase caused by the higher plasma density, preventing a positive feedback which would make the system unstable.

Additional evidence for a nonlinear increase in the plasma loss rate is found by examining the magnetospheric response to the outburst. Previous observations have noted that the plasma torus appears offset toward the dawn direction (*16*). This effect is a predicted consequence of a large-scale dawn-dusk electric field of about 4 mV m^{-1} across the inner magnetosphere (*17*). The field is thought to be due to the $\mathbf{v} \times \mathbf{B}$ electric field, where $\mathbf{v}$ is the plasma velocity and $\mathbf{B}$ is the jovian magnetic field strength, set up by the plasma flowing down the magnetotail, with the field propagated to the inner magnetosphere in a manner analogous to terrestrial equatorial currents.

Our preoutburst observations of the plasma torus show this expected dawn offset: the peak of emission intensity on the dusk side occurred at 5.4 R_J, whereas the dawn peak occurred at 5.6 R_J. During the outburst, the peaks of emission of the plasma torus shifted even further dawnward. This shift was most prominent on the dawn side and only marginally visible on the dusk side. The dawnward shift of the plasma torus increased with each increase in the plasma mass (Fig. 4A) (*18*).

A dawnward shift in the plasma torus can be caused by an increase in the large-scale electric field across the inner magnetosphere. Such an increase could be caused by an increase in the plasma outflow and thus by an increase in mass loss from the plasma torus. The transition between where the magnetospheric motion is dominated by corotation and radial transport and where the tailward flow begins occurs around a characteristic distance, the Hill length L_H, of (*19*)

$$L_H = \left(\frac{\pi \Sigma R_J^2 B_J^2}{\dot{M}}\right)^{1/4} \qquad (1)$$

where Σ is the Pederson conductivity of the jovian ionosphere (the conductivity in the direction of the electric field), B_J is the jovian surface magnetic field strength, and $\dot{M}$ is the total rate of outward mass transport. As $\dot{M}$ increases, L_H decreases, and tailward flow begins closer to Jupiter. Closer to Jupiter, the magnetic field strength B is

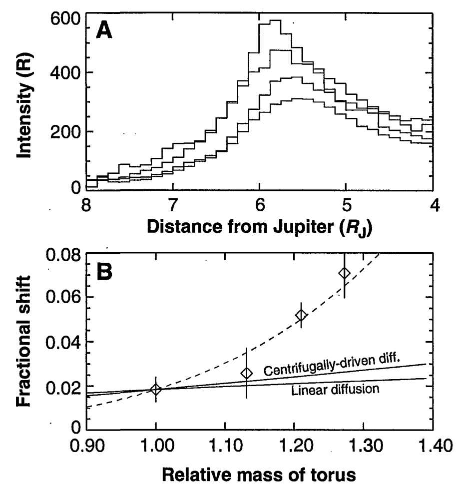

Fig. 4. Shifts in the plasma torus. (**A**) The dawnside emission intensity profile at four time periods before and during the torus perturbation. The torus shifts systematically dawnward with the increase in mass. (**B**) The peak of torus emission as a function of relative torus mass for the four time periods above. Also plotted are the shifts expected for plasma transport by simple diffusion and by centrifugally driven diffusion, using the model in Eq. 2. The dashed line is the best fit, where plasma outflow is proportional to the seventh power of the mass of the plasma torus.

higher, and for a simple dipole, the strength goes as $B \propto 1/R_J^3$. Thus, the tailward plasma flow begins in a region of stronger magnetic field, and, assuming that the tailward flow velocity is controlled by the solar wind speed and remains constant, the electric field E, which is proportional to $\mathbf{v} \times \mathbf{B}$, increases as

$$E \propto \dot{M}^{3/4} \qquad (2)$$

This analysis reproduces the basic expected behavior of the relationship between changing plasma outflow rates and the large-scale electric field: An increase in the mass outflow will cause an increase in the electric field, thus a dawnward shift in the Io plasma torus, as observed (20).

The dawnward shift, and thus the plasma outflow rate, increases as the mass of the plasma torus increases. This behavior is that expected of a loss-limiting mechanism stabilizing the interaction between Io and the magnetosphere. From Eq. 2 and the measured shift in the plasma torus, we can estimate the plasma outflow rate as a function of the plasma mass. The best polynomial fit to the data is given by a model where plasma outflow is proportional to the seventh power of the plasma mass (Fig. 4B) (21). We place no significance on the specific polynomial fit; the critical characteristic suggested by these data is that plasma outflow increases quickly with an increase in plasma mass. Even the nonlinearity of centrifugally driven diffusion cannot account for the increase in plasma outflow with increasing plasma mass. Another even more nonlinear mechanism, such as transport through large-scale plasma instability (10), is required in this case.

We now estimate the magnitude of the outburst from Io. In a purely loss-limited system, perturbations to the neutral cloud mass directly reflect perturbations to the source from Io, so the increase in Na directly reflects the Na increase of the source. But is the mass increase in Na, a minor species in the neutral cloud, indicative of the behavior of the dominant S and O? The subsequent increase in the S plasma mass following the Na outburst shows that atomic S must have increased in mass at the same time as atomic Na, but the total amount of the S increase remains unknown. We calculated a lower limit to the atomic S increase by assuming the minimum plasma outflow consistent with the observed loss-limited behavior, given by centrifugally driven diffusion. Using the model of the interaction between the neutral cloud and plasma torus (Fig. 1) (22), we found that a small perturbation, such as that seen in the plasma torus, requires a mass input increase of about the same amount as the perturbation. Thus, for the minimal plasma outflow, the 30% increase in plasma torus mass requires a 30% increase in neutral cloud mass. As the Na mass increases by a factor of ~2, Na would have to be ~7 times overabundant in the outburst compared to S in this case.

Assuming, however, that the much larger increase in plasma outflow with increased plasma mass inferred from the plasma torus shift is correct, a much larger atomic S increase is required to account for the increase in S plasma mass. For this case, we find that the observed 30% increase in plasma torus mass requires an increase of a factor of ~3 in supply to the neutral cloud, in agreement with the increase by a factor of ~2 in the neutral Na cloud mass. Thus, the data are consistent with the hypothesis that the mass of Na is a direct tracer of the mass of the more dominant S (and presumably O) components.

It is not possible to directly determine the cause of the increase in gas supply from Io, but with volcanic activity a known transient phenomenon on the satellite, the eruption of a volcanic plume on the satellite is a natural explanation (23). A typical plume should affect the supply rate by only a small amount, however: Voyagers 1 and 2 imaged nine active plumes on Io (4). All plumes except one, however, were active during both Voyager encounters—4 months apart—so short-term variability is not necessarily expected for these plumes. Pele, the largest observed plume, was the only one observed to have turned off between the Voyager 1 and 2 encounters. Thus, it appears that the largest plumes are the most variable, and that a plume with duration of only ~70 days (Fig. 2) might be expected to be a large Pele-like outburst. If the neutral cloud is fed by sputtering of atmospheres local to active plumes, the contribution of each individual plume should be roughly proportional to the surface area covered by the plume. Based on Voyager measurements of observed plume widths (4), the surface area covered by Pele was almost four times greater than the surface area covered by all of the other plumes taken together. Thus, the increase by a factor of 2 or more in the supply of Na to the neutral cloud suggested by the data would be expected for the largest observed plumes on Io (22).

The following scenario explains the observations we present. Starting on about day 680, a large plume, with dimensions similar to those of the Pele plume, began erupting. This eruption greatly increased the surface area of plume material available to be sputtered into the neutral cloud, and the neutral cloud mass quickly adjusted to this increase in mass input. The plume remained active for about 70 days, and its output was variable during this time. The increase in mass of the neutral cloud caused an increase in the supply of ions to the plasma torus, so the mass of the plasma torus began to increase. The increase in mass of the plasma torus then led to a highly nonlinear increase in plasma outflow, causing the plasma torus mass to fall to its equilibrium value quickly after the cessation of plume activity.

This scenario suggests the following implications for Io and the plasma torus: (i) The stability of the magnetosphere-Io interaction is controlled not by Io and the details of its atmosphere and mass pickup, but by the magnetosphere and the method of plasma transport. (ii) An increase in plasma mass causes a very strong increase in plasma loss from the torus. (iii) Sodium is a good tracer of plume activity on Io. (iv) The large response of the Na neutral cloud, if it is representative of the S and O clouds, shows that the Io atmosphere is easily overwhelmed by the eruption of a single large plume, lending support to the idea that the atmosphere of Io arises primarily from plumes (24). (v) Variable volcanic activity on Io affects plasma mass, plasma transport, and large-scale electric fields in the jovian magnetosphere.

REFERENCES AND NOTES

1. D. B. Nash, M. H. Carr, J. Gradie, D. M. Hunten, C. F. Yoder, in *Satellites*, J. A. Burns and M. S. Matthews, Eds. (Univ. of Arizona Press, Tucson, 1986), pp. 629–688.
2. See review by J. R. Spencer and N. M. Schneider [*Annu. Rev. Earth Planet. Sci.* **24**, 125 (1996)].
3. H. M. Moos, T. E. Skinner, S. T. Durrance, M. C. Festou, J. L. Bertaux, *Astrophys. J.* **294**, 369 (1985); N. Thomas, *J. Geophys. Res.* **98**, 18737 (1993).
4. R. G. Strom and N. M. Schneider, in *Satellites of Jupiter*, D. Morrison, Ed. (Univ. of Arizona Press, Tucson, 1982), pp. 598–533.
5. See review by N. M. Schneider, M. A. McGrath, and W. H. Smyth [in *Time Variable Phenomena in the Jovian System*, M. J. S. Belton *et al.*, Eds. (NASA SP-494, 1989), pp. 75–99].
6. A. F. Cheng, *J. Geophys. Res.* **93**, 12751 (1988).
7. R. E. Johnson and M. McGrath, *Geophys. Res. Lett.* **20**, 1735 (1993).
8. See, for example, J. K. Wilson and N. M. Schneider, *J. Geophys. Res.*, in press.
9. G. L. Siscoe and D. Summers, *ibid.* **86**, 8471 (1981).
10. D. H. Pontius and R. A. Wolf, *Geophys. Res. Lett.* **17**, 49 (1990); Y. S. Yang, R. A. Wolf, R. W. Spiro, T. W. Hill, A. J. Dessler, *J. Geophys. Res.* **99**, 8755 (1994).
11. Light from a slit 6 arc min long by 10 arc sec wide was passed through the spectrograph and dispersed to a resolution of $\lambda/\Delta\lambda$ of ~40,000, about 0.015 nm. The slit was centered on the position of Jupiter and aligned with either the plasma torus plane, for observations of plasma torus ion emissions, or the Io orbital plane, for observations of the extended neutral cloud. The 6 arc min extent of the slit gave a spatial resolution of about 0.1 R_J for a distance of about 9 R_J on the east (dawn) and 9 R_J on the west (dusk) side of Jupiter (An R_J is a jovian radius, 7.14×10^4 km). Each of the 382 observations consisted of a 40-min charge-coupled device integration centered at a wavelength of either 672.5 nm, to record the plasma torus S^+ emission lines at 671.7 and 673.1 nm, or 589.0 nm, to record the extended neutral cloud Na lines at 588.9 and 589.6 nm. Details on the observations and the plasma torus data reduction can be found in M. Brown [thesis, University of California at Berkeley (1994)]. Reduction of the Na data followed essentially the same

techniques, with additional complications due to the Na night-sky lines, the continuum spectrum of Io, and the water absorption features.

12. F. Bagenal, *J. Geophys. Res.* **99**, 11043 (1994).
13. To examine the long-term behavior of the plasma torus intensities, we removed short-term periodic modulations in the S^+ emission. The two observed modulations in the data occur at periods of 9.925 hours (the System III rotational period of Jupiter) and 10.214 hours {an unexplained modulation termed "System IV" [B. R. Sandel and A. J. Dessler, *ibid.* **93**, 5487 (1988)]} [M. E. Brown, *ibid.* **100**, 21683 (1995)]. The measured intensities are divided by the sliding-average of the modulation at these periods to remove the variations of about 30 and 40% for System III and IV, respectively. The emission intensity of S^+ is proportional to the product of the electron and ionized S densities, (approximately proportional to the square of the S^+ density), as the emission is due to the electron impact excitation of the S. Analysis of the emission intensities from the neutral Na cloud suffers the complication that the emission seen is from the resonant scattering of sunlight; the emission intensity thus depends on the received solar flux at the wavelength of the atomic transition, and therefore, on the heliocentric velocity of the Na atoms [J. T. Bergstralh, J. W. Young, D. L. Matson, T. V. Johnson, *Astrophys. J.* **211**, L51 (1977); R. A. Brown and Y. L. Yung, in *Jupiter*, T. Gehrels, Ed. (Univ. of Arizona Press, Tucson, 1976), pp. 1102–1145]. This effect is dependent mostly on Io's orbital phase, so we correct by removing the sliding-average modulation of the data at Io's orbital period. The total modulation by Io phase is 50%.
14. We estimated the total mass increase in the plasma torus by summing all emission along the slit and taking the square root, as the emission intensity is proportional to the product of the ion density and the electron density, which we assume scale together. Figure 2 appears to imply an even larger change in mass only because of the structural changes that occur in the torus at the same time.
15. An alternative scenario might be envisioned where the increase in mass of the neutral Na cloud is caused by an increase in the Na lifetime caused, for example, by a decrease in the electron temperature. We reject this hypothesis for two reasons: (i) Observations of the plasma torus, while not directly sensitive to electron temperature, show no change in the plasma torus mass, ion temperature, or rotation velocity at the start of the neutral Na cloud perturbation, and (ii) the increase in mass of the plasma torus shows that for S, at least, the supply increases precisely when the Na mass increases, strongly suggesting that the Na mass increase is caused by a Na supply increase.
16. C. B. Pilcher, J. H. Fertel, J. S. Morgan, *Astrophys. J.* **207**, 181 (1980); A. J. Dessler and B. R. Sandel, *Geophys. Res. Lett.* **19**, 2099 (1992); N. M. Schneider and J. T. Trauger, *Astrophys. J.* **450**, 450 (1995).
17. D. D. Barbosa and M. G. Kivelson, *Geophys. Res. Lett.* **10**, 210 (1983).
18. The lack of a shift on the duskside is unexpected. If the electric field operates uniformly across the magnetic field both sides should shift equally. The exclusively dawnside shift suggests that the electric field variations occur only on the dawn, explaining these data and also the sporadic dawnside shifts observed in imaging data (*16*).
19. T. W. Hill, *J. Geophys. Res.* **84**, 6554 (1979). Voyager measurements show that $L_H \sim 20\ R_J$.
20. We are indebted to A. J. Dessler for the analogy to terrestrial equatorial currents and for the suggestion of the form of the relationship between an increasing plasma outflow and an increasing electric field.
21. The data were grouped into four groups for determination of the emission peak. The groups correspond to (in order of faintest to brightest) preoutburst (days 580 through 689), increasing phase of outburst (days 690 through 700), declining phase of outburst (days 723 through 750), and peak of outburst (days 700 through 722) periods. The fractional torus shift is defined as $(p_{\mathrm{dawn}} - p_{\mathrm{dusk}})/(p_{\mathrm{dawn}} + p_{\mathrm{dusk}})$, where p_{dawn} and p_{dusk} are the position of the peak of plasma torus intensity on the dawn and dusk sides, respectively. As above, the relative density is estimated by the square root of the total intensity integrated along the spectral slit. The theoretical curves are calculated assuming zero electric field for a zero mass plasma torus and by forcing the curves to go through the equilibrium mass point (relative torus mass of 1.0).
22. The models of the behavior of the neutral cloud and magnetosphere mass are based on the zero-dimensional models of T. S. Huang and G. L. Siscoe [*J. Geophys. Res.* **91**, 10163 (1986)]. For the supply-limited case, supply to the neutral cloud is proportional to the square root of the plasma density, and diffusive loss from the magnetosphere is proportional to the plasma density. For the loss-limited case, supply to the neutral cloud is proportional to the plasma density, and loss from the magnetosphere is proportional to the fourth power of the plasma density. For both cases, model input parameters are adjusted to yield a steady-state plasma lifetime of 30 days and a neutral lifetime of 20 hours.
23. Direct imaging of a new plume at the time of the outburst would provide conclusive proof of this hypothesis, but the capability of obtaining such an image was not available at the time of these observations. Ground-based infrared observations are able to monitor hotspot activity on Io, but we have no reason to expect that these are associated with plumes on Io, nor were any observations obtained during the outburst [G. J. Veeder, D. L. Matson, T. V. Johnson, D. L. Blaney, J. D. Goguen, *ibid.* **99**, 17095 (1994)].
24. See, for example, E. Lellouch, *Icarus* **124**, 1 (1996).
25. W. H. Smyth and M. R. Combi, *Astrophys. J.* **328**, 888 (1988).
26. D. F. Strobel, in (*5*), pp. 183–195.
27. We benefited greatly from conversations with A. J. Dessler, T. W. Hill, M. A. McGrath, E. J. Moyer, and D. H. Pontius. This research would not have been begun without a generous seed grant from the California Space Institute and would not have proceeded without the reliable help of A. Misch and the other staff at Lick Observatory.

6 May 1997; accepted 12 August 1997

Organics and Other Molecules in the Surfaces of Callisto and Ganymede

T. B. McCord,* R. W. Carlson, W. D. Smythe, G. B. Hansen, R. N. Clark, C. A. Hibbitts, F. P. Fanale, J. C. Granahan, M. Segura, D. L. Matson, T. V. Johnson, P. D. Martin

Five absorption features are reported at wavelengths of 3.4, 3.88, 4.05, 4.25, and 4.57 micrometers in the surface materials of the Galilean satellites Callisto and Ganymede from analysis of reflectance spectra returned by the Galileo mission near-infrared mapping spectrometer. Candidate materials include CO_2, organic materials (such as tholins containing C≡N and C–H), SO_2, and compounds containing an SH-functional group; CO_2, SO_2, and perhaps cyanogen [$(CN)_2$] may be present within the surface material itself as collections of a few molecules each. The spectra indicate that the primary surface constituents are water ice and hydrated minerals.

The four largest satellites of Jupiter, called the Galilean satellites after their discoverer, are a mini solar system. They are about moon-sized to larger than Mercury, and the innermost satellite, Io, is the most volcanically active body in the solar system. Europa, the second Galilean satellite from Jupiter, has a dense core and an ice crust that may be underlain by a liquid water ocean. Ganymede, the third Galilean satellite, is also differentiated, with scars from giant impacts but clearly showing essentially complete resurfacing. Finally, Callisto, the fourth satellite, appears heavily cratered and undifferentiated, thus perhaps preserving evidence of its early history (*1*). The Galilean satellites are located in the temperature region of the solar system where water ice and other volatiles become stable over the age of the solar system (*2*). The composition and chemistry of the surfaces of these objects is of interest because they provide clues to the origin of our solar system and because they contain water ice and may contain organic molecules that are essential for the initiation of life.

The NASA Galileo spacecraft carried the near-infrared mapping spectrometer (NIMS) (*3*) into orbit around Jupiter on 7 December 1995, and the NIMS started spectrometric observations of the Galilean satellites in June 1996 (*4*, *5*). The NIMS covers the wavelength range 0.7 to 5.2 μm with up to 408 spectral channels and a resolving power of 40 to 200 ($\Delta\lambda/\lambda$, where λ is wavelength). The instrument's instantaneous field of view is 0.5 mrad, giving a spatial resolution (pixel size) of, for example, 5 km at a distance of 10,000 km. The

T. B. McCord, G. B. Hansen, C. A. Hibbitts, F. P. Fanale, P. D. Martin, Hawaii Institute of Geophysics and Planetology, University of Hawaii, Honolulu, HI 96822, USA.
R. W. Carlson, W. D. Smythe, M. Segura, D. L. Matson, T. V. Johnson, Jet Propulsion Laboratory, Pasadena, CA 91109, USA.
R. N. Clark, U.S. Geological Survey, Denver, CO 80225–0046, USA.
J. C. Granahan, Science and Technology International, Incorporated, Honolulu, HI 56813, USA.

*To whom correspondence should be addressed. E-mail: tom@kahana.pgd.hawaii.edu